Molecular Crystals and Liquid Crystals Science and Technology. Section A. Molecular Crystals and Liquid Crystals

Publication details, including instructions for authors and subscription information:
http://www.tandfonline.com/loi/gmcl19

Novel Electrical and Optical Properties of Liquid Crystals Infiltrated in Opal as Photonic Crystal

Katsumi Yoshino [a], Yuki Shimoda [a], Keizo Nakayama [a], Tatsuhiko Tamura [a], Tatsunosuke Matsui [a], Hirotake Kajii [a] & Masanori Ozaki [a]

[a] Department of Electronic Engineering, Graduate School of Engineering, Osaka University, 2-1 Yamada-Oka, Suita, Osaka, 565-0871, Japan

Version of record first published: 24 Sep 2006

To cite this article: Katsumi Yoshino, Yuki Shimoda, Keizo Nakayama, Tatsuhiko Tamura, Tatsunosuke Matsui, Hirotake Kajii & Masanori Ozaki (2001): Novel Electrical and Optical Properties of Liquid Crystals Infiltrated in Opal as Photonic Crystal, Molecular Crystals and Liquid Crystals Science and Technology. Section A. Molecular Crystals and Liquid Crystals, 364:1, 501-509

To link to this article: http://dx.doi.org/10.1080/10587250108025020

Mol. Cryst. and Liq. Cryst., 2001, Vol. 364, pp. 501-509
Reprints available directly from the publisher
Photocopying permitted by license only

Novel Electrical and Optical Properties of Liquid Crystals Infiltrated in Opal as Photonic Crystal

KATSUMI YOSHINO, YUKI SHIMODA, KEIZO NAKAYAMA, TATSUHIKO TAMURA, TATSUNOSUKE MATSUI, HIROTAKE KAJII and MASANORI OZAKI

Department of Electronic Engineering, Graduate School of Engineering, Osaka University, 2–1 Yamada-Oka, Suita, Osaka 565–0871, Japan

Various liquid crystals can be infiltrated into interconnected nanosize voids in a three-dimensional periodic array of SiO_2 spheres, synthetic opals, as photonic crystals. As an example of tunable photonic crystals, it has been demonstrated that the optical stop band in transmission spectrum of the liquid crystal infiltrated opal shifts with changing temperature, which can be interpreted in terms of temperature dependence of the refractive index and confirmed by the theoretical calculation of the band structure. This phenomenon can be utilized as a method to evaluate the refractive index. Tunability of optical properties of photonic crystal is also demonstrated in infiltrated replicas of opals. Effects of electric field application on properties of the infiltrated opals are also clarified.

Keywords: photonic crystal; opal; stop band; nematic liquid crystal; ferroelectric liquid crystal

INTRODUCTION

Recently, photonic crystals [1,2] with a three-dimensional ordered structure of a periodicity of optical wavelength, have attracted considerable attention from both fundamental and practical viewpoints, since new physical concepts such as a photonic band gap have been theoretically deduced and various application of photonic crystals have been proposed.

We have demonstrated that the three-dimensional periodic structure of silica particles, which is named synthetic opal, can be realized by a self-assembly method, that is, by sedimentation of nanoscale SiO_2 spheres of the order of optical wavelength range [3].

We have also proposed to realize new functionality by infiltrating various materials into interconnected nanoscale voids of the synthetic opals and indicated various interesting phenomena. [3-10] In addition, we have proposed a tunable

photonic crystal in which the photonic band gap can be tuned as desired by controlling parameters such as periodicity, space filling fraction, refractive index and so on. The infiltrated opal should be one of candidates to realize such a tunable photonic crystal.

In this study, we demonstrate tunability of optical properties in opals infiltrated with liquid crystals. Electrical properties of the liquid crystal infiltrated opal are also discussed.

EXPERIMENTAL

Synthetic opals with a three-dimensional mesoscopic periodic structure as photonic crystals were fabricated by sedimentation of the suspension of mono-dispersed SiO_2 spheres. To study the effect of applied electric field, thin opal films were formed by sedimentation of mono-dispersed silica spheres in sandwich cells made of two glass [or InSn oxide (ITO) glass] plates with separation of various thickness [7]. In this paper, the opals fabricated from SiO_2 spheres of 300nm, 550nm and 1μm in diameter are named opal-300, opal-550 and opal-1000, respectively.

Optical stop band in the transmission spectrum was observed in the visible range for the case of opals made of mono-dispersed SiO_2 spheres in the range of 150~300nm in diameter. Opals prepared with SiO_2 spheres of 550-nm and 1-μm diameters exhibited stop bands in the infrared range. Polymer opals were also prepared with polymer spheres of the order of several hundred nm in diameter.

Various organic materials can be infiltrated in the periodic array of percolated pores of the opal. Replicas of opals can be prepared by dipping the infiltrated opals in HF and dissolving silica particles.

Liquid crystals can be infiltrated in the isotropic phase upon heating. Nematic liquid crystal ZLI1132 (Merck) and smectic liquid crystal (R)-4'-(1-methoxycarbonyl-ethoxy)phenyl-4-[4-(n-octyloxy)phenyl]benzoate (1MC1EPOPB) were used for infiltration [11].

Transmission spectra through opal films were measured with a Hitachi 330 spectrophotometer and a FT-IR spectrometer (FT/IR-300E, JASCO). Reflection spectra were measured using a hand-made experimental setup with a W lamp as a light source and a multichannel spectrometer (PMA-11, Hamamatsu Photonics) as a detector. The microphotograph of scanning electron microscope (SEM) was taken with a S-2100C Hitachi microscope.

Theoretical calculations of opals and liquid crystal infiltrated opals were carried out using a plane wave method [12]. In this paper, we consider a fcc-closed packed structure of SiO_2 spheres with a refractive index n=1.46 and assume a filling ratio of f = 0.74 of SiO_2 spheres.

FIGURE 1 The electron microphotograph of the opal film fabricated from SiO_2 spheres of 300nm in diameter

RESULTS AND DISCUSSION

Figure 1 shows an electron microphotograph of the opal film made of SiO_2 spheres of 300nm in diameter. This opal film exhibits beautiful opalescent colors, and a clear peak in the reflection spectrum and a stop band in the transmission spectrum were observed depending on the diameter of SiO_2 spheres.

Figures 2 and 3 show the transmission spectra of the opal-300 and the opal-300 infiltrated with the nematic liquid crystal ZLI1132 and smectic liquid crystal 1MC1EPOPB, respectively. It should be noted in these figures, both stop bands shift upon the infiltration of the liquid crystal. In addition, stop bands shift also with changing temperature. As is evident in the insets of these figures, especially at the phase transition point, the stop band shifts in step wise.

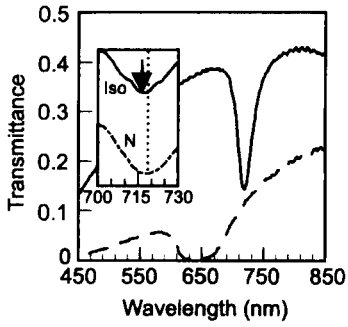

FIGURE 2 Transmission spectra of the opal-300 (dashed line) and opal-300 infiltrated with ZLI1132. Inset shows transmission spectra of infiltrated opal-300 as a function of temperature.

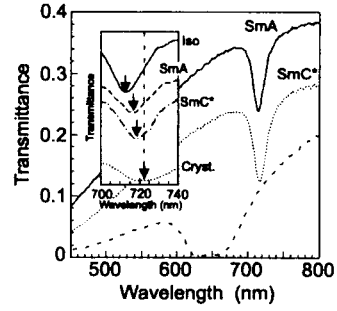

FIGURE 3 Transmission spectra of the opal-300 (dashed line) and opal-300 infiltrated with 1MC1EPOPB at various phases. Inset shows transmission spectra of infiltrated opal-300 as a function of temperature.

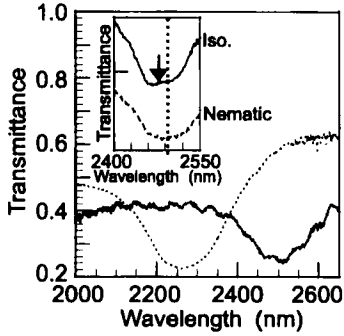

FIGURE 4 Transmission spectra of the opal made of 1μm SiO_2 spheres (dotted line), and the opal infiltrated with nematic liquid crystal (ZLI1132).

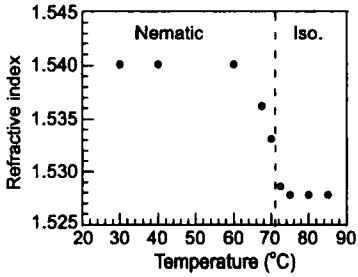

FIGURE 5 Temperature dependence of evaluated refractive index of nematic liquid crystal (ZLI1132) in voids of opals made of 300nm SiO_2 spheres.

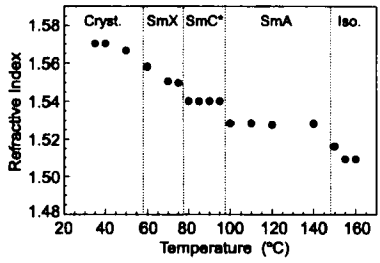

FIGURE 6 Temperature dependence of evaluated refractive index of smectic liquid crystal (1MC1EPOPB) in voids of opals made of 300nm SiO_2 spheres.

As shown in Fig.4, the stop band and its shift with the infiltration of the liquid crystal were observed in the infrared spectral range in the case of the opal-1000.

These spectral shifts of the stop band can be interpreted in terms of the change in refractive index with temperature. From a simple analysis of Figs. 2 and 3 using the evaluated periodicity, temperature dependences of the refractive index in ZLI1132 and in 1MC1EPOPB were evaluated as shown in Figs. 5 and 6. Remarkable change in the refractive index at the phase transition was clearly confirmed.

The shifts of the stop band and the reflection peak were also clearly observed in

the opal replica upon liquid crystal infiltration. It should be mentioned that the infiltration effect to the band shift was even larger in the replicas compared with that in original opal, as shown in Fig.7.

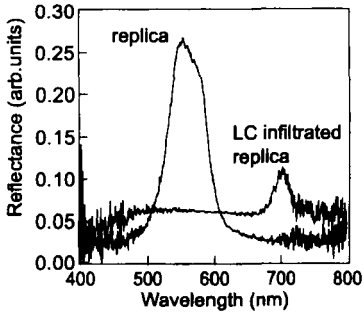

FIGURE 7 Reflection spectra of pure polymer replica and polymer replica infiltrated with the nematic liquid crystal.

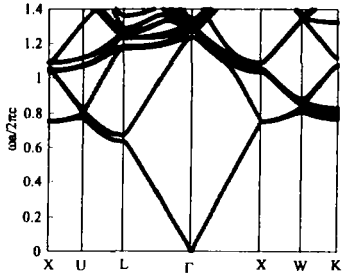

FIGURE 8 Band structure for the silica opal (n=1.46) in air.

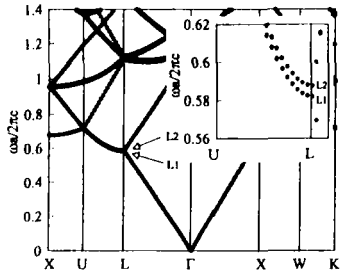

FIGURE 9 Band structure for the liquid crystal (n=1.54) infiltrated opal. Inset: expanded band structure near the L point.

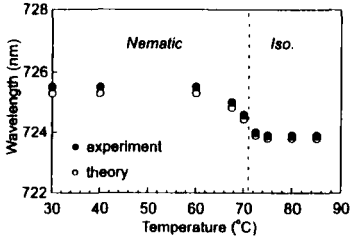

FIGURE 10 Temperature dependence of evaluated center wavelength of stop band of nematic liquid crystal (ZLI1132) in voids of opal and the center wavelength between the first and second bands estimated from the theoretical calculation.

The band structures of the silica opal and liquid crystal infiltrated opal were theoretically calculated using a plane wave method. Figures 8 and 9 show the

calculation results of the band structure for the original silica opal in air and the liquid crystal infiltrated opal, respectively. As is evident from these figures, the gap between first and second bands appears at the L point corresponding to the light propagation perpendicular to (1,1,1) plane, and the central frequency between first and second bands at the L point shifts to lower energy (longer wavelength) upon infiltration of the liquid crystal. Temperature dependence of the center wavelength between the first and second bands estimated from the theoretical calculation is indicated in Fig. 10, which coincides well with the experimental results.

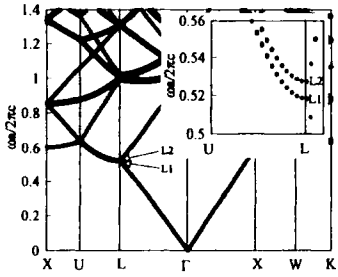

FIGURE 11 Band structure for the polymer opal (n=1.7) infiltrated with liquid crystal (n=1.54). Inset: expanded band structure near the L point.

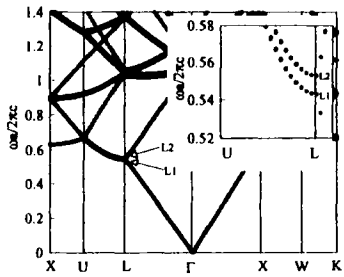

FIGURE 12 Band structure for the polymer replica (n=1.7) infiltrated with liquid crystal (n=1.54). Inset: expanded band structure near the L point.

Figures 11 and 12 indicate the theoretical band structures for a polymer opal infiltrated with the liquid crystal and a polymer replica infiltrated with the liquid crystal, which clearly indicates that the replica exhibits larger shift upon liquid crystal infiltration in accordance with the experimental result.

These results mentioned above clearly indicate that a temperature tunable photonic crystal can be realized by liquid crystal infiltrated photonic crystal.

It should also be noted that the observation of shift of the stop band or the reflection peak in opal upon infiltration is one of the simple methods to evaluate the refractive index. Therefore, we checked this method by applying to various liquids. Figure13 indicates the transmission spectra of the polymer opal replica infiltrated with various organic liquids. As is evident in the inset of Fig.13, the center wavelength of the stop band is a linear function of the refractive index of the infiltrated liquids.

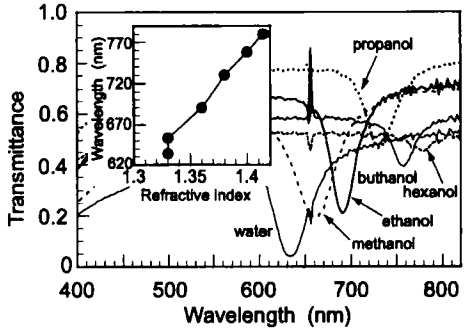

FIGURE 13 Transmission spectra of the polymer opal replica infiltrated with various organic liquids. Inset shows the stop band wavelength as a function of the refractive index of liquids.

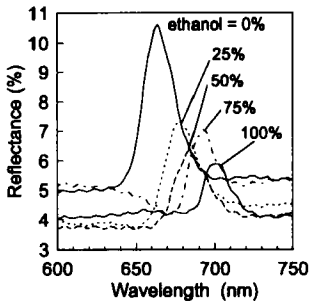

FIGURE 14 Reflection spectra of the opal infiltrated with methanol-ethanol mixture at various concentration of the ethanol in the mixture.

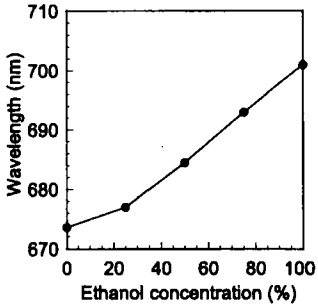

FIGURE 15 The center wavelength of the reflection peak of the opal infiltrated with the methanol-ethanol mixture as a function of the ethanol concentration in the mixture.

Figure14 shows the reflection peak in the polymer opal replica infiltrated with methanol-ethanol mixture. It should be noted that the reflection peak wavelength depends on the solvent. Figure.15 shows the ethanol concentration dependence of the wavelength of the reflection peak in the polymer opal replica infiltrated with the methanol-ethanol mixture. As is evident from this figure, the reflection peak markedly shifted by changing ethanol concentration in the mixture. This phenomenon was reversible. These spectral change should originate from the difference in refractive index. In this case, however, the change in the periodicity of the polymer opal replica due to the swelling of the polymer by the solvent must also be taken into account for the detailed interpretation of the change of the spectra. In any case, it has been demonstrated that the stop band can be controlled by the concentration of the mixed

solvents. We can also propose the measurement of concentration of the mixture by this simple method.

We have also studied effect of applied voltage on the transmission spectra of the opals infiltrated with the nematic liquid crystal and also smectic liquid crystal. However, the shift of the stop band was small. This may be due to the effect of strong interaction of liquid crystal molecules with the inner surface of the void in opal.

The study of the stop band and the reflection peak in the liquid crystal infiltrated opal which are prepared with larger spheres and pretreated with surfactant to reduce interaction at the surface, and also replica are now under progress.

The study on a dielectric behavior in the liquid crystal infiltrated opal has also been carried out. Figure 16 shows a frequency dispersion of dielectric constant of ZLI1132 in a conventional sandwich cell and in the nanoscale voids of the opal-300. The relaxation frequency of the nematic liquid crystal infiltrated in the opal evaluated from the Cole-Cole analysis shown in Fig.16(b) is higher than that in the sandwich cell shown in Fig.16(a). This may be attributed to the strong interactions of liquid crystals with the inner surface of the nano-scale voids in the opal.

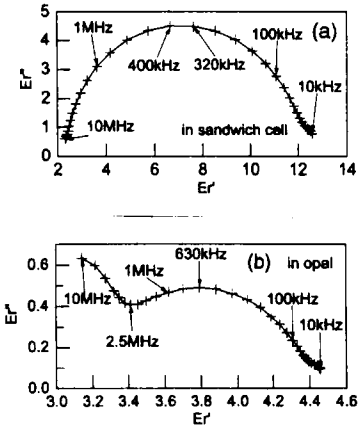

FIGURE 16 Frequency dispersion of dielectric constant of ZLI1132 in a conventional sandwich cell (a) and in the nanoscale voids of opal (b).

Similar surface effect to the molecular dynamics in the opal voids was observed in the temperature dependence of dielectric constant of 1MC1EPOPB. At the transition temperature between the smectic-A (SmA) and chiral smectic C (SmC*) phases, a sharp peak appeared in the temperature dependence of dielectric constant in the

sandwich cell, which is interpreted to be associated with the soft mode relaxation. In the infiltrated system in the opal, however, the sharp peak was not observed. In general, the Goldstone mode of the dielectric relaxation in the SmC* phase is strongly influenced by the surfaces and is suppressed in a thin sandwich cell [13,14]. The disappearance of the sharp peak at the Curie point observed in this study may suggest that even soft mode contribution is suppressed in the nanoscale spaces in the opal.

SUMMARY

Optical properties of synthetic opal and opal replica infiltrated with the liquid crystal and liquids were investigated and we demonstrated that the stop bands of the opal and replica could be tuned by changing temperature, which was confirmed by the theoretical calculation. These results strongly support the possibility of the tunable photonic crystals.

Acknowledgements

We would like to express our sincere thanks to New Energy and Industrial Technology Development Organization (NEDO) by reporting that part of the work was supported by NEDO International Joint Research Grant. Part of this study was carried out as Cooperative Research of Creation and Education of Novel Characteristics of Nano-size Molecular System supported by Fund of Research for the Future of the Japan Society for the Promotion of Science (Project No. JSPS-RFTF96P00206).

References

[1] S. John, Phys. Rev. Lett. **58**, 2486 (1987).
[2] E. Yablonovitch, Phys. Rev. Lett. **58**, 2059 (1987).
[3] K. Yoshino, K. Tada, M. Ozaki, A. A. Zakhidov and R. H. Baughman, Jpn. J. Appl. Phys. **36**, L714 (1997).
[4] K. Yoshino, S. Tatsuhara, Y. Kawagishi, M. Ozaki, A. A. Zakhidov and Z. V. Vardeny, Jpn. J. Appl. Phys. **37**, L1187 (1998).
[5] K. Yoshino, S. Tatsuhara, Y. Kawagishi, M. Ozaki, A. A. Zakhidov and Z. V. Vardeny, Appl. Phys. Lett. **74**, 2590 (1999).
[6] K. Yoshino, S. Satoh, Y. Shimoda, Y. Kawagishi, K. Nakayama and M. Ozaki, Jpn. J. Appl. Phys. **38**, L961 (1999).
[7] K. Yoshino, Y. Shimoda, Y. Kawagishi, K. Nakayama and M. Ozaki, Appl. Phys. Lett. **75**, 932 (1999).
[8] S. Satoh, H. Kajii, Y. Kawagishi, A. Fujii, M. Ozaki and K. Yoshino, Jpn. J. Appl. Phys. **38**, L1475 (1999).
[9] K. Yoshino, H. Kajii, Y. Kawagishi, M. Ozaki, A. A. Zakhidov and R. H. Baughman, Jpn. J. Appl. Phys. **38**, 4926 (1999).
[10] H. Kajii, Y. Kawagishi, H. Take, K. Yoshino, A. A. Zakhidov and R. H. Baughman, J. Appl. Phys. **88**, 758 (2000).
[11] H. Taniguchi, M. Ozaki, K. Yoshino, K. Satoh and N. Yamasaki, Ferroelectrics **77**, 137 (1988).
[12] K. -M. Ho, C. T. Chan and C. M. Soukoulis, Phys. Rev. Lett. **65**, 3152 (1990).
[13] K. Yoshino, M. Ozaki, H. Agawa and Y. Shigeno, Ferroelectrics **58**, 283 (1984).
[14] K. Yoshino, K. Nakao, H. Taniguchi and M. Ozaki, J. Phys. Soc. Jpn., **56**, 4150 (1987).